High Melting Point of Linear, Spiral Polyethylene Nanofibers and Polyethylene Microspheres Obtained Through Confined Polymerization by a PPM-Supported Ziegler-Natta Catalyst

Yu Xiao,[a] Xiying Dai,[a] Kui Wang,*[b] and Guangyuan Zhou*[b]

In this work, different types of polyethylene (linear, spiral nanofibers and microspheres) were obtained via confined polymerization by a PPM-supported Ziegler-Natta catalyst. Firstly, the Ziegler-Natta catalyst was chemical bonded inside the porous polymer microspheres (PPMs) supports with different pore diameter and supports size through chemical reaction. Then slightly and highly confined polymerization occurred in the PPM-supported Ziegler-Natta catalysts. SEM results illustrated that the slightly confined polymerization was easy to obtain linear and spiral nanofibers, and the nanofibers were observed in polyethylene catalyzed by PPMs-1#/cat and PPMs-2#/cat with low pore diameter (about 23 nm). Furthermore, the highly confined polymerization produced polyethylene microspheres, which obtained through other PPM-supported Ziegler-Natta catalysts with high pore diameter. In addition, high second melting point (T_{m2}: up to 143.3 °C) is a unique property of the polyethylene obtained by the PPM-supported Ziegler-Natta catalyst after removing the residue through physical treatment. The high T_{m2} was ascribed to low surface free energy (σ_e), which was owing to the entanglement of polyethylene polymerized in the PPMs supports with interconnected multimodal pore structure.

1. Introduction

Polyolefin, as one of the most important polymer materials, has been widely used in many industries and human life, resulting in greatly improvement of people's livelihood and life quality.[1] In order to break the barriers between laboratory and industry, and promote the large-scale industrial production of polyolefin, polyolefin catalyst needs to be supported on the carriers. There are several advantages for the supporting catalysts: i) the catalytic activity could be improved effectively; ii) it could meet the requirements of existing industrial facilities well; iii) the morphology and apparent density of polyolefin products could be improved; iv) the use of co-catalysts could be greatly reduced, thereby reducing production costs.[2] With further research on catalyst supports, the field of the catalyst supports has been expanded form original inorganic $MgCl_2$ to multiple types and scales, such as molecular sieve, carbon nanotube, polystyrene, etc.[3]

In recent decades, with the rapid development of nanotechnology, it is found that the structure of polymer materials changed at the nanometer scale, and this phenomenon has drawn wide attention in the academic field.[4] According to the researches, the molecular chain structure, condensed matter structure, phase structure and stability of polymers will change at nanoscale, leading to quite different properties of polymers compared with the bulk state.[4e,5] Therefore, the concept of polymerization in a nano-confined space (defined as confined polymerization) has been proposed by scientists. Here the active center is loaded inside the supports, and then polymerization occurs in the nano space, hoping to obtain the product with different structure and performance compared with corresponding bulk product. After that, the goal, controlling the structure of polymer at different scales, could be achieved.[4c,5f,6]

Aida and co-workers[4a] chose mesoporous silicon fiber (MSF) as a carrier to support Cp_2TiCl_2 catalyst, then ethylene was polymerized in the MSF support. Moreover, the pore diameter of MSF was 2.7 nm with uniform pore structure. During the polymerization process, polyethylene molecular chains did not fold but to grow along the axis parallel to the MSF pores, because the 2.7 nm pore diameter was much smaller than the thickness of polyethylene crystal lamellar. Hence, polyethylene nanofibers with a straight chain structure and high melting point and ultrahigh molecular weight were finally obtained. According to this study, the concept of nano-extruder and extrusion polymerization in nanopores were proposed. After that, a number of attempts to polymerize olefin in the nano-confined space have been made. Choi et al.[7] used anodic aluminium oxide (AAO) film with the diameter of 60 nm

[a] Dr. Y. Xiao, Dr. X. Dai
State Key Laboratory of Advanced Power Transmission Technology
Global Energy Interconnection Research Institute
No.18 Binhe Avenue, Changping District, Beijing, 102209, (P. R. China)
[b] Dr. K. Wang, Prof. G. Zhou
Key Laboratory of Polymer Ecomaterials
Changchun Institute of Applied Chemistry (CIAC), Chinese Academy of Sciences (CAS)
No. 5625 Renmin Rd., Changchun, Jilin 130022, (P. R. China)
E-mail: wangkui0512@163.com
gyzhou@dicp.ac.cn

Supporting information for this article is available on the WWW under https://doi.org/10.1002/open.202000290

as a template to carry Cp*Ti(OCH_3)$_3$ for styrene polymerization. After confined polymerization, polystyrene fibers with high molecular weight (M_w = 928.000 g/mol) and high melting point were synthesized. According to the study of Liu et al.,[8] the preparation of polyethylene nanofibers requires a durable confined space, and the weakening or disappearance of confined space is not conducive to generate fibers. Although there are many researches on the confined polymerization of inorganic supports, some defects are still exist: i) the active center could be deactivated by the inorganic supports; ii) the supports will remain as inorganic ash in the product; iii) the polymerization by the inorganic supported catalyst can't provide an environment that is similar to homogeneous polymerization. Therefore, developing a kind of organic support for confined polymerization is urgent.

Roscoe et al.[2a,c] synthesized polystyrene microspheres with nanopores through copolymerization, and then the polystyrene microspheres were used as supports for olefin polymerization. The results demonstrated that polymerization occurred independently in each polystyrene microspheres. Since then, more and more porous polymer supports were obtained for olefin confined polymerization. Uemura et al.[4b,9] studied the effects of porous polymer supports channels on polymerization activity, molecular weight and structure. It was found that chain termination was effectively suppressed when the polymerization was carried out inside the pores. The obtained polystyrene represented a low molecular weight distribution and high isotacticity. In our previous work, three catalysts, Cp_2ZrCl2, Cp_2TiCl_2, and Ziegler-Natta, were supported into porous polymer microspheres (PPMs) (pore diameter: 9.0 nm), which was designed and synthesized all by ourselves, for ethylene confined polymerization.[10] The results indicated that three different confined polymerization (highly confined polymerization, slightly confined polymerization, and non-confined polymerization) occurred in the confined space of PPMs. Here highly confined polymerization was defined as the supports were gradually expanded rather than broken up during polymerization process, and the supports could provide continuous confined space for the whole polymerization. Slightly confined polymerization was defined as the supports were broken up gradually, and the supports could provide confined space part of polymerization process. Non-confined polymerization means that the supports could not provide any confined space for the polymerization process. However, most of the studies, including our previous work, were concentrated on the effect of porous polymer supports with a particular pore diameter on the confined polymerization. Based on the literature,[8] polymerizing in inorganic supports with different nanopores could obtain various products. Hence, changing pore diameter of the porous polymer supports with interconnected pores and better toughness might result in more complicated phenomena compared with that of inorganic supports.

In this article, two types of PPMs with different pore diameter and supports size were synthesized. After that, Ziegler-Natta catalysts were supported inside PPMs followed by ethylene polymerization. The aims of this context are those: i) Firstly, studying the effect of PPMs with different structures on confined polymerization activity; ii) Secondly, figuring out the variation of the structure and properties of confined polymerization products under the influence of PPMs supports structure changes.

2. Results and Discussion

2.1. Structure Data of the PPMs Supports and Ti Contents of the PPM-Supported Catalyst

The pore structure data of PPMs supports and corresponding Ti loading amounts are illustrated in Table 1. As shown, the PPMs supports can be divided into two types according to the variation of pore diameter and supports size: i) one is the similar pore diameter (around 22–23 nm) and different supports size (10.30 and 7.68 μm), i.e., PPMs-1# and PPMs-2#; ii) the other is the increasing pore diameter (from 23.3 to 86.3 nm) and similar size of PPMs supports (approximate 7 μm), i.e., PPMs-2#, PPMs-3# and PPMs-4#. The Ti contents of PPM-supported catalysts were measured by ICP-OES, and the loading amounts of Ti are around 6 wt% (Table 1). The SEM images of PPMs before and after Ziegler-Natta catalyst loading are listed in Figure 1. It is found that spherical structure of PPMs supports is maintained after Ziegler-Natta catalyst loading, and the size of PPMs changes little.

Then, the pore structure spectra of PPM-supported Ziegler-Natta catalysts are illustrated in Figure 2. Obviously, the interconnected tri-modal pore structure is still existed inside PPM-supported Ziegler-Natta catalysts. Figure 2a–d shows that the pore size distribution of the tri-modal pore structure is mainly between 3–10 nm and 20–70 nm. The unique tri-modal pore structure is caused by PPMs supports, which were formed

Table 1. Pore structure data[a] of PPMs supports and corresponding Ti contents of PPM-supported catalysts.

Sample	S_{BET}/m^2/g	d_p/nm	S_p/μm	V_p/cm^3/g	Ti/wt%
PPMs-1#	56.21	22.6	10.30	0.183	6.12
PPMs-2#	48.90	23.3	7.68	0.152	6.31
PPMs-3#	7.28	48.0	7.22	0.022	6.80
PPMs-4#	0.60	86.3	7.26	0.003	6.21

[a] The BET specific surface area (S_{BET}), average pore diameter (d_p), and specific pore volume (V_p), were measured from BJH adsorption data, and average size of PPMs (S_p) was obtained from SEM images.

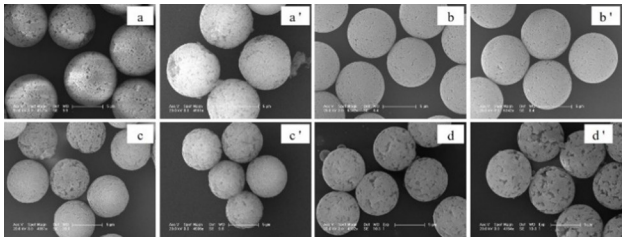

Figure 1. SEM images of PPMs-1# (a), PPMs-1#/Cat (a'), PPMs-2# (b), PPMs-2#/Cat (b'), PPMs-3# (c), PPMs-3#/Cat (c'), PPMs-4# (d), and PPMs-4#/Cat (d').

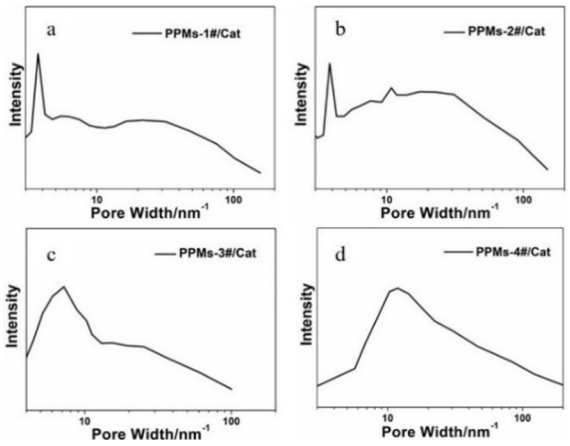

Figure 2. The pore size distributions for PPM-supported catalysts

through the copolymerization of acrylonitrile, polystyrene and 1,4-divinylbenzene.

FTIR and XPS were used to study the connection between Ziegler-Natta catalysts and PPMs supports. As shown in Figure 3a, reduced intensity of cyano groups and increasing intensity of imine groups indicate that chemical reaction occurred between activating agents (CH_3MgCl) and cyano groups. It is the chemical reaction that transformed the cyano groups into imine groups. The chemical reaction was also confirmed by the increasing characteristic peak of N_{1s} binding energy (from 399.0 eV to 399.6 eV) after adding the activating agents (CH_3MgCl) in Figure 3b.[11] Furthermore, Figure 3c indicates that the binding energies of $Ti_{2p3/2}$ and $Ti_{2p1/2}$ for the PPM-supported Ziegler-Natta catalyst are 458.5 and 464.3 eV, respectively. The two values of $Ti_{2p3/2}$ and $Ti_{2p1/2}$ are higher than that of homogeneous $TiCl_4$ catalyst in the literature,[12] indicating the formation of cationic active species through chemical reaction. Therefore, the results of FTIR and XPS show that Ziegler-Natta catalyst and PPMs supports are connected by chemical bonding. Hence, the preparation mechanism of PPM-supported Ziegler-Natta catalysts could be deduced, as shown in Figure 3d.

As mentioned above, Ziegler-Natta catalysts are supported into the two types PPMs supports through chemical bonding. In addition, the spherical structure with interconnected multi-modal nanopore is still maintained after Ziegler-Natta catalysts loading in the PPMs, which could provide a confined space for ethylene polymerization.

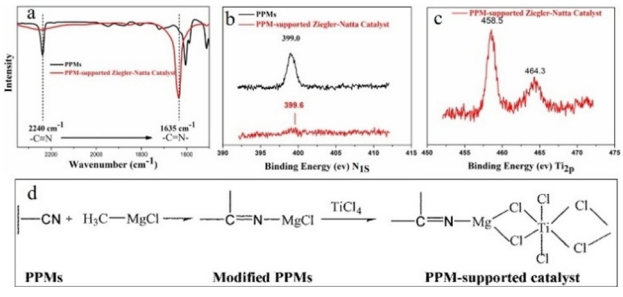

Figure 3. FTIR (a), XPS (b–c) spectra and the preparation mechanism (d) of PPM-supported Ziegler-Natta catalysts

2.2. Ethylene Confined Polymerization

Then ethylene polymerization was catalyzed by the PPM-supported Ziegler-Natta catalysts with different structure. The mechanism of the confined polymerization and corresponding polymerization results are shown in the following Figure 4 and Table 2, respectively.

As shown in Table 2, the PPM-supported Ziegler-Natta catalysts with larger support size (PPMs-1#) has higher polymerization activity, when using PPM-supported Ziegler-Natta catalysts with similar pore diameter and different supports size, i.e., PPMs-1# and PPMs-2#. For instance, the activity of PE-6# is 567.8 kg PE/(mol of Ti h MPa), which is higher than that of PE-13# (276.5 kg PE/(mol of Ti h MPa)). This phenomenon is reasonable because the S_{BET}, average size and V_p of PPMs-1# and PPMs-2# are different, even though they own similar average pore diameter. The larger S_{BET}, average size and V_p of area, the easier contact between ethylene monomer and Ti active center, leading to an increasing polymerization activity.

It can be seen that the PPMs-3# supported Ziegler-Natta catalyst with the pore diameter of 48.0 nm has the highest polymerization activity among the three kinds of PPMs supports (PPMs-2#, PPMs-3# and PPMs-4#), when the PPMs supports size are similar and the pore diameter increases from 23.3 to 86.3 nm. For example, the activity of PE-17# is 930.4 kg PE/(mol of Ti h MPa), which is higher than PE-15# (865.9 kg PE/(mol of Ti h MPa)) and PE-23# (778.7 kg PE/(mol of Ti h MPa)).This result is attributed to three reasons: i) the polyethylene produced in nanopores will block the pores and hinder subsequent polymerization when the pore diameter is too small, leading to a low polymerization activity; ii) the specific surface area is small if the pore diameter is too large, and then the Ti active centers can't fully contact with ethylene monomer, resulting in the reduction of the polymerization activity; iii) the concentration of co-

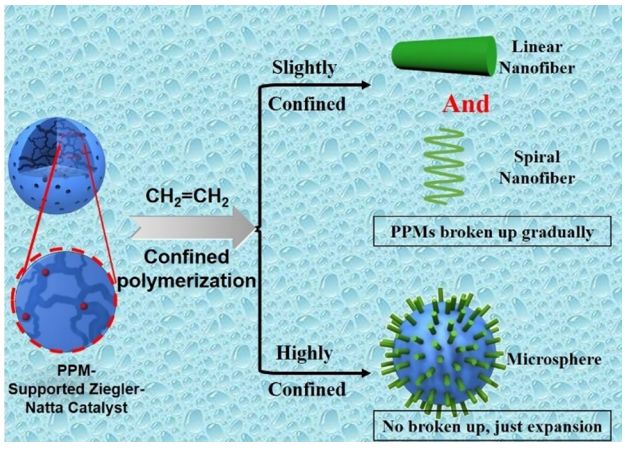

Figure 4. The mechanism of confined polymerization occurred in PPM-supported catalyst.

Table 2. Various results of confined polymerizations with different PPM-supported Ziegler-Natta catalysts.

Support	Run	Ti Content/ μmol	Al/ Ti	Pressure/ MPa	Temperature/ °C	Time/ min	Yield/ g	Activity[a]	T_{m1}[b]/ °C	X_c%	T_{m2}[c]/ °C	X_c%	T_c/ °C	M_w[d]	PDI
PPMs-1#	PE-1#	20.3	200	0.5	50	30	5.36	1057.6	140.2	60	137.5	54	114.2	17.23	2.44
	PE-2#	23.6	670	0.5	50	30	5.81	983.0	139.4	58	138.7	56	112.7	7.75	2.06
	PE-3#	30.4	490	0.3	46	30	3.64	798.4	140.2	62	137.8	53	113.5	7.74	1.71
	PE-4#	30.4	490	0.9	49	30	7.86	574.9	139.1	62	137.0	58	114.6	22.73	3.44
	PE-5#	30.4	490	0.3	51	15	1.12	493.2	140.9	62	140.2	57	113.1	9.56	2.10
	PE-6#	30.4	490	0.5	32	30	2.59	567.8	144.3	61	138.4	47	112.9	12.02	1.65
	PE-7#	30.4	490	0.5	52	30	4.23	557.4	139.0	65	137.9	64	113.4	12.40	2.71
PPMs-2#	PE-8#	30.6	300	0.5	50	30	4.55	595.4	139.4	57	135.6	52	114.8	11.52	1.86
	PE-9#	30.6	490	0.5	50	30	5.18	676.8	141.7	64	138.3	57	116.5	22.71	2.28
	PE-10#	30.6	600	0.5	50	30	4.92	642.6	142.0	59	137.4	56	113.3	23.63	2.62
	PE-11#	30.6	490	0.3	50	30	3.14	684.9	139.8	61	135.0	51	115.5	14.82	2.00
	PE-12#	30.6	490	0.7	50	30	6.59	615.5	139.6	72	136.5	67	114.4	12.78	2.15
	PE-13#	30.6	490	0.5	30	30	2.12	276.5	143.4	65	136.8	49	113.2	10.92	1.83
	PE-14#	30.6	490	0.5	50	30	4.30	561.7	141.2	59	137.3	56	114.9	27.39	3.09
	PE-15#	27.2	660	0.5	50	30	5.89	865.9	141.4	70	136.9	61	113.0	6.78	1.68
PPMs-3#	PE-16#	26.4	300	0.5	50	30	6.43	975.8	140.2	58	136.8	54	113.1	12.09	2.62
	PE-17#	26.4	600	0.5	50	30	6.13	930.4	140.1	62	138.1	60	111.2	7.41	2.60
	PE-18#	26.4	610	0.3	50	30	3.89	984.4	138.7	55	136.0	55	112.8	22.23	2.48
	PE-19#	26.4	610	0.7	50	30	5.58	604.3	140.0	57	136.3	50	111.7	15.92	2.52
	PE-20#	26.4	610	0.5	30	30	4.89	741.1	140.7	67	136.4	56	111.4	56.02	2.53
	PE-21#	26.4	610	0.5	49	30	6.38	967.6	138.4	64	136.6	59	112.7	32.16	3.80
PPMs-4#	PE-22#	25.1	300	0.5	50	30	5.25	837.6	138.6	66	136.1	63	113.7	9.80	2.01
	PE-23#	25.1	600	0.5	50	30	4.88	778.7	140.5	59	137.3	55	113.5	10.64	2.10
	PE-24#	25.1	800	0.3	50	30	2.37	630.8	139.4	65	135.4	60	113.8	10.44	1.93
	PE-25#	25.1	800	0.7	50	30	5.77	657.6	138.3	61	135.2	57	114.5	11.30	2.28
	PE-26#	25.1	600	0.5	30	30	3.21	511.7	141.3	64	133.6	51	112.6	34.41	1.87
	PE-27#	25.1	600	0.5	49	30	6.15	980.5	138.7	68	135.3	57	114.2	26.15	2.60

Polymerization condition: in a 0.1 L autoclave, 60 ml hexane; [a] kgPE/(mol of Ti h MPa); [b] first melt of DSC scan; [c] second melt of DSC scan; [d] weight-average molecular weight (M_w): $\times 10^4$ g (mol PE)$^{-1}$

catalyst Triethyl Aluminium (TEA) was high in the large pore diameter, also increasing the probability of Ti active centers that transferred to the TEA chain, which could also reduce the polymerization activity; iV) What is more, PPMs-3# samples have the highest Ti concentration than others, leading to the highest activity than other PPM-supported catalyst. Therefore, we can deduce that only the proper pore diameter of PPMs supports is conducive to the release of activity, and PPMs-3# supported catalyst is the best among the above three supported catalysts (PPMs-2#, 3# and 4#).

2.3. Micromorphology of Obtained Polyethylene

Figure 5 illustrates the micromorphology of polyethylene obtained by confined polymerization of PPM-supported Ziegler-Natta catalysts. A large number of polyethylene microspheres are clearly observed in Figure 5a, and the particle sizes of these microspheres are between 60–100 μm. Moreover, the microspheres structure can be observed in all the products prepared by the four kind PPM-supported Ziegler-Natta catalysts. The surface of these microspheres is magnified to further analyze their structure. As shown in Figure 5a′–a′′, the microspheres are composed of multiple nanofibers with the diameter of 100 nm, which are similar to the morphology of polyethylene obtained in our previous study.[10] The same morphology of polyethylene indicates that confined polymerization also can be occurred in the nanopores with the diameter of 23.3 to 86.3 nm.

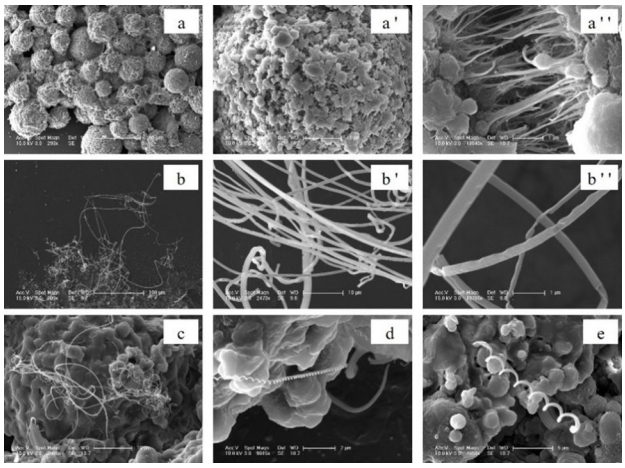

Figure 5. SEM micrographs of polyethylene prepared by PPM-supported Ziegler-Natta catalysts in different morphology. (a–a′′) polyethylene microspheres observed in polyethylene by all the four PPM-supported catalysts, (b–e) linear and spiral polyethylene nanofibers which observed in the polyethylene with high T_{m2} by PPMs-1#/cat and PPMs-2#/cat. (Figure 2a′, a′′, b′ and b′′ are the magnification images of Figure 2a and Figure 2b, respectively)

It is an interesting phenomenon that is also appeared in SEM images, as illustrated in Figure 5b-d. Individual linear nanofibers (Figure 5b–c) and spiral nanofibers (Figure 5d–e) are observed in the polyethylene catalysed by PPMs-1#/cat and PPMs-2#/cat, in addition to the typical polyethylene microspheres composed of nanofibers (Figure 5a–a′′). The Linear and

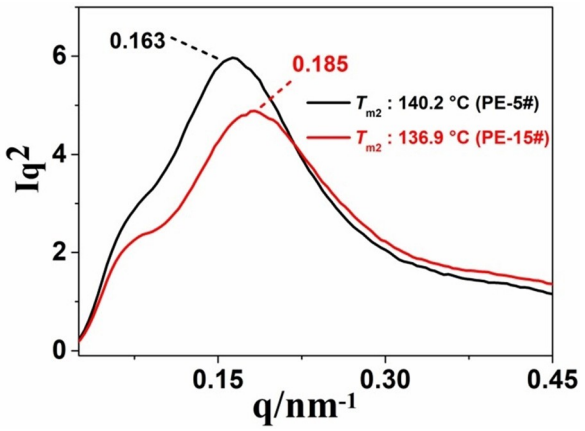

Figure 7. The one-dimensional SAXS data of the initial obtained polyethylene with different T_{m2}.

spiral polyethylene nanofibers are not observed in the highly confined polymerization in our previous research.[10] This phenomenon is not surprising after further analysis, and it is also reasonable. On the basis of our previous research, confined polymerization could be divided into slightly confined (defined as the supports were broken up gradually, and the supports could provide confined space part of polymerization process) and highly confined (defined as the supports were gradually expanded rather than broken up during polymerization process, and the supports could provide continuous confined space for the whole polymerization). The former resulted in polyethylene nanofibers, while the latter led to polyethylene microspheres. Different morphology of the obtained polyethylene was caused by different initial polymerization activity of Cp_2TiCl_2 and Ziegler-Natta catalysts. The initial polymerization activity of Cp_2TiCl_2 was high, and the generated polyethylene would be broken into nanofibers gradually. While the activity of Ziegler-Natta catalysts was gentle, the obtained polyethylene would be polymerized in PPMs and the spherical structure was maintained during the process. However, the gentle activity of Ziegler-Natta does not mean that all of the PPM-supported catalysts were not broken up during the polymerization process. In this work, the PPMs with the lowest pore diameter (PPMs-1# and PPMs-2#: about 23 nm) exhibit more possibility to be broken up gradually. The reason of this phenomenon is that the low pore diameter makes the PPMs supports suffer from more pressure during polymerization process than the PPMs with high pore diameter. Thus, the PPMs-1#/cat and PPMs-2#/cat may not afford the expansibility of polymerization, then the polyethylene would be broken and generated nanofibers gradually (Figure 5b–e), which is similar to PPM-supported Cp_2TiCl_2 catalysts.

As for the formation of linear and spiral nanofibers, this is attributed to the unique nanopore structure of PPMs support (Figure 2). The structure of our supports is the interconnected multi-modal pore, which is different from traditional inorganic supports (such as SBA-15 and carbon nanotube). Here the pore is formed from the crosslinking of styrene and 1,4-divinylbenzene, leading to the ordered nanopores, as well as some disordered channels interconnected with each other. Therefore, the linear nanofibers will be produced through the ordered nanopores, and the spiral nanofibers are generated from the disordered channels.

2.4. Different T_{m2} of Initial Obtained Polyethylene

There are also significant differences in the melting point of the initial obtained polyethylene (especially the secondary melting point, T_{m2}), besides various surface morphology. Most of the primary melting point of initial obtained polyethylene is higher than 140 °C, which is the characteristic of confined polymerization.[4a,7] However, the T_{m2} of the initial obtained polyethylene have changed after eliminating thermal history. The polyethylene with linear and spiral nanofibers are still higher than 138 °C, which was polymerized by PPMs-1#/cat and PPMs-2#/cat (low pore diameter).The T_{m2} of polyethylene with microspheres structure are reduced to135 °C, and they were obtained through PPM-supported catalysts with high pore diameter. This phenomenon has not been observed before, and the thermal properties we tested were the polyethylene that removing the residue of catalyst and the matrix through physical method in the previous research.[10]

Two kinds of initial obtained polyethylene with different T_{m2} (PE-15#: 136.9 °C and PE-5#: 140.2 °C) were chosen with the purpose of studying the difference between them. First of all, their structures are analyzed, and the obtained data are demonstrated in Figure 6. It can be seen from Figure 6a that the initial obtained polyethylene with different T_{m2} are orthorhombic crystal, and the characteristic peaks are located at ≈21° and 24°. In Figure 6b, there is only the characteristic peak of methylene at 30 ppm, indicating that the obtained polyethylene are linear polyethylene. That is to say, there is no significant difference in the structure of the polyethylene with different T_{m2}. (PE-15#: 136.9 °C and PE-5#: 140.2 °C).

As we all know, melting point (T_m) is affected by the thickness of lamellar (d_c) and surface free energy (σ_e), and the relationship between them could be analyzed by the Gibbs-Thompson equation. As a result, SAXS was used to study the crystallization of polyethylene with different T_{m2}, and one-dimensional SAXS profiles and corresponding data are illustrated in Figure 7 and Table 3, respectively. Here the amorphous layers thicknesses (d_a) and the thickness of lamellar (d_c) of polyethylene were calculated from DSC and SAXS results.

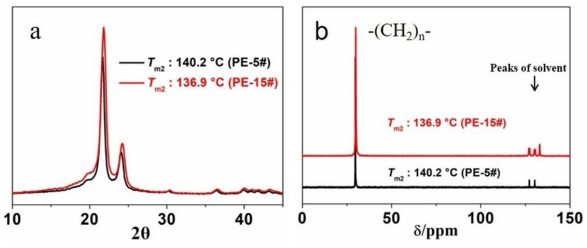

Figure 6. The XRD spectra (a) and ^{13C} NMR spectra (b) of the initial obtained polyethylene.

Table 3. The T_{m2}, d_{ac}, d_c and d_a of the initial obtained polyethylene with different T_{m2}.

Run	T_{m2}/°C	q	d_{ac}[a]/nm	X_c%	d_c[b]/nm	d_a[c]/nm
PE-5#	140.2	0.163	38.5	57	21.9	16.6
PE-15#	136.9	0.185	33.9	61	20.7	13.2

[a] $d_{ac}=2\pi/q$; [b] $d_c=d_{ac}{}^{*}X_c$; [c] $d_a=d_{ac}-d_c$

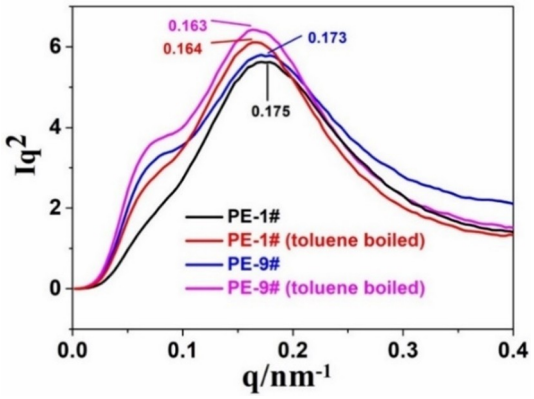

Figure 9. The one-dimensional SAXS data of the polyethylene before and after removing residue.

$$T_m = T_m^0\left(1-\frac{2\sigma_e}{d_c\Delta H_f^0}\right) \quad (1)$$

In equation (1) the equilibrium melting point is represented by T_m^0, and the enthalpy of fusion per unit volume is symbolized by ΔH_f^0. According to our calculation, there is a difference (about 1.2 nm) in the d_c of the two kinds of polyethylene. The thicker of d_c is, the higher value of T_{m2} is. Therefore, it can be concluded that the difference in d_c of polyethylene results in various T_{m2}.

2.5. Further analysis of polyethylene with high T_{m2} after physical treatment

According to the research in section 2.4, it is found that polythene obtained through highly confined polymerization exhibits different values of T_{m2} (from 135 °C to 140 °C), and this result is different from our previous results.[10] The T_{m2} of the polythene we obtained before was high (up to 143.8 °C),[10] and

Table 4. Thermal properties of polyethylene before and after removing residue through physical method.

Run	T_{m1}/°C	X_c %	T_{m2}/°C	X_c %	T_c/°C
PE-1#	140.2	60	137.5	54	114.2
PE-1# (toluene boiled)	144.3	68	143.3	61	108.2
PE-9#	141.7	64	138.3	57	116.5
PE-9# (toluene boiled)	140.8	70	142.5	61	108.8
PE-28# (SBA-15/Ziegler-Natta Catalyst)	143.0	62	135.8	47	117.2
PE-28#(SBA-15/Ziegler-Natta Catalyst, toluene boiled)	137.2	48	137.6	33	114.3

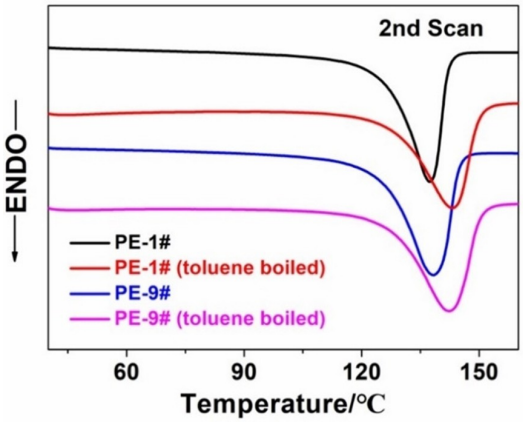

Figure 8. DSC spectra of polyethylene before and after removing residue through physical method.

the high T_{m2} polythene (143.8 °C) was treated through physical method before DSC test, in order to eliminate the effect of residue (catalyst and the matrix) on thermal performance. The same physical treatment of polythene obtained in this work was chosen to further analyze the difference between the previous and present work, and the corresponding treatment process is illustrated in Experimental section. Here the two samples we chosen show low T_{m2} (138.3 and 137.5 °C), and polythene prepared by SBA-15-supported Ziegler-Natta catalyst (T_{m2}:135.8 °C) is also selected for comparison.

Table 4 and Figure 8 demonstrate the variation of the thermal performance of polyethylene before and after removing residue through physical method. As shown in Table 4, the T_{m2} of polyethylene prepared by PPM-supported catalyst increases significantly, from 137.5 to 143.3 °C, while that by SBA-15-supported catalyst only increases 1.8 °C (T_{m2}: 137.6 °C). This changing indicates that the real thermal performance of the as-prepared polyethylene is inhibited by the residue, which existed in the initial obtained polyethylene. The characteristic of highly confined polymerization, high T_{m2}, will appear after removing the residue, and the high T_{m2} is consistent with our previous work.

SAXS test for the polyethylene was also conducted and the result was analyzed. As can be seen from Figure 9 and Table 5, the value of q decreases by about 0.01 after removing residue through physical treatment (from 0.17 to 0.16), after that the values of d_c and d_a are calculated based on DSC result. In Table 5, the d_c of both two polyethylene increase to about 23.4 nm, while there is a little decrease in d_a from 15.6 to 15.0 nm, indicating that the increasing T_{m2} is attributed to the thicker d_c after removing residue.

It is found that the products exhibit the high T_{m2} (up to 143.3 °C) after removing residue through physical treatment, which are not observed in other researches.[4a,5f,6d] According to the literatures,[13] the constant values of T_m^0 and ΔH_f^0 are 145.5 °C and 280 J/cm^3, respectively, and theoretical value of σ_e is 90×10^{-7} J/cm^2. After that, the value of d_c could be calculated based on these values (Equation 1), and the results are illustrated in Table 6.

Table 5. The d_c and d_a of the polyethylene before and after removing residue.

Run	T_{m2}/°C	q	d_{ac}[a]/nm	X_c%	d_c[b]/nm	d_a[c]/nm
PE-1#	137.5	0.175	35.9	54	19.4	16.5
PE-1# (toluene boiled)	143.3	0.164	38.3	61	23.4	14.9
PE-9#	138.3	0.173	36.3	57	20.7	15.6
PE-9# (toluene boiled)	142.5	0.163	38.5	61	23.5	15.0

[a] $d_{ac}=2\pi/q$; [b] $d_c=d_{ac}* X_c$; [c] $d_a=d_{ac}-d_c$

Table 6. The d_c obtained through different ways.

Run	T_{m2}/°C	d_c/nm (obtained through SAXS result)	d_c/nm (calculated based on equation 1)
PE-1# (toluene boiled)	143.3	23.4	42.5
PE-9# (toluene boiled)	142.5	23.5	31.2

In comparison with the d_c obtained by SAXS result through our polymerization, the d_c calculated based on equation 1 is much higher, which is a very interesting phenomenon. The huge difference in the two values of d_c by different methods indicate that one of the values in equation 1 is not constant, and it is the uncertain value that causes the big deviation of d_c. Coming back to equation 1, there is only σ_e, which is just a theoretical value. Therefore, the key factor of high T_{m2} is the reduction of σ_e rather than the increasing d_c. As described in Section 2.1, the supports (PPMs) exhibit unique structure with interconnected multi-modal nanopores, leading to more entanglement of polyethylene prepared by confined polymerization compared with traditional supports (SBA-15, CNTs), and then generate fewer chain ends.[10] In the process of heating, a large number of entangled chains and fewer chain ends can reduce the value of σ_e, resulting in high T_{m2}.[14] Results showed that the high T_{m2} is the inherent property of polyethylene prepared by PPM-supported Ziegler-Natta catalyst, which is attributed to the unique interconnected multi-modal pore structure of the PPMs supports.[10,15]

3. Conclusion

In this work, linear, spiral polyethylene nanofibers and polyethylene microspheres were prepared via slightly and highly confined polymerization by PPM-supported Ziegler-Natta catalyst, respectively. DSC data of the initial obtained polyethylene showed that the residue (catalyst and the matrix) had an adverse effect on the thermal properties of polyethylene (especially the T_{m2}), and the high T_{m2} (up to 143.3 °C) emerged after removing the residue through physical treatment. After the physical treatment, the thickness of lamellar (d_c) increased, but this is not the main reason for increasing T_{m2} (from 137.5 °C to 143.3 °C). Based on our study, the key factor to high T_{m2} is the low σ_e, which is ascribed to the entanglement of polyethylene synthesized in the PPMs supports with interconnected multi-modal pore structure. Furthermore, the high T_{m2} was the unique feature for the polyethylene confined polymerization by PPM-supported Ziegler-Natta catalyst.

Experimental Section

Materials

The materials used in this work and syntheses of porous polymer microspheres (PPMs) supports with different pore structure are illustrated in the Supporting Information.

Preparation of the PPM-Supported Ziegler-Natta Catalyst

All experiments that sensitive to air and moisture were using the standard Schlenk technique in nitrogen condition.

First of all, PPMs supports were activated to remove moisture and air in a vacuum oven for 12 h at 60 °C. CH_3MgCl and a certain weight of PPMs were mixing in 60 mL toluene, then the mixture were stirred at 50 °C for 4 h. After that, the obtained product was filtered, washing the obtained solid with toluene more than three times. Then, adding 60 mL toluene and $TiCl_4$ in the washed solid, the mixture was stirred at 50 °C for 4 h followed by filtered again. At last, the obtained solid was washed five times with toluene, and then the solid was vacuum dried at room temperature.

Ethylene Polymerization

Ethylene slurry polymerization by PPM-supported Ziegler-Natta catalysts was polymerized in a 0.1 L autoclave stainless steel reactor. The steel reactor contains mechanical stirring and inlets for adding catalyst and ethylene monomer. First of all, the steel reactor was heated to 80 °C and then cooled down to setting temperature under vacuum. Then TEA was added into the steel reactor under inert gas. After stirring a few minutes the PPM-supported Ziegler-Natta catalyst solution was added into the steel reactor. Then the setting pressure of ethylene monomer was injected to start ethylene confined polymerization. After certain minutes, the polymerization was terminated by acidified ethanol. Then polyethylene product was obtained and then vacuum dried.

Physical Treatment of Initial Obtained Polyethylene

The purpose of physical treatment is to eliminate the effect of residue (catalyst and the matrix) on thermal performance. Firstly, initial obtained polyethylene was wrapped by filter paper. Then put them into the inner device with pores in its wall. Toluene and a little antioxidant were added into the assembled device (Figure S1 in the Supporting Information). Subsequently, this device was

refluxing for 5–6 h at 130 °C with magnetic stirring. Since polyethylene is soluble in toluene at high temperature, while the PPMs (cross-linked polystyrene) and catalysts are not. It is only polyethylene that could penetrate through the filter paper, leaving the matrix and the catalyst in the filter paper.

Characterization

The surface areas (S_{BET}), average pore diameter (d_p), pore volume, and specific pore volume (V_p) of porous polymer microspheres (PPMs) support and corresponding PPM-supported Ziegler-Natta catalysts were measured by a specific surface area physisorption apparatus, and the model was NOVA-1000, USA. The Ti active center contents of the PPM-supported catalysts were obtained through an ICP-OES, and the model was Thermo iCAP 6000, USA. SEM pictures of PPMs supports, corresponding PPM-supported catalysts and polyethylene were observed by a FESEM, and the model was Philips XL30 ESEM, Netherlands. The structure of polyethylene was tested by an XRD, and the model was Brucker D8, Germany, a SAXS (France, Xenocs) and ^{13}C-NMR (Germany, Bruker DPX-300). Thermal properties of polyethylene before and after physical treatment were measured by a DSC (Switzerland, Mettler Toledo) at 10 °C/min from 30 °C to 190 °C. Molecular weight (M_w) and molecular weight distribution (PDI) of polyethylene were measured by a gel permeation chromatography (GPC, USA, PL-GPC 220).

Acknowledgements

This study is supported by the State Key Laboratory of Advanced Power Transmission Technology (Grant No. GEIRI-SKL-2018-012), Natural Science Foundation of Zhejiang (No. LQ19E030007).

Conflict of Interest

The authors declare no conflict of interest.

Keywords: confined polymerization · polyethylene · spiral nanofibers · microspheres · Zigler-Natta catalysts

[1] a) J. Tellers, A. Zych, P. Neuteboom, M. Soliman, J. Vachon, *Eur. Polym. J.* **2020**, *131*, 109721 ; b) J. Dai, H. C. Luo, M. Moloney, J. Qiu, *ACS Appl. Mater. Interfaces* **2020**, *12*, 22019–22028; c) W. Wang, Y. Liu, Z. Q. Han, Q. Wang, *Polym. Degrad. Stab.* **2020**, *174*, 109093 ; d) H. Zhang, Y. Meng, Y. F. Cao, Y. Yao, D. L. Fan, T. Z. Yang, T. Qian, *Nanotechnology* **2020**, *31*, 8.

[2] a) S. B. Roscoe, J. M. J. Frechet, J. F. Walzer, A. J. Dias, *Science* **1998**, *280*, 270–273; b) G. Fink, B. Steinmetz, J. Zechlin, C. Przybyla, B. Tesche, *Chem. Rev.* **2000**, *100*, 1377–1390; c) S. B. Roscoe, C. Gong, J. M. J. Fréchet, J. F. Walzer, *J. Polym. Sci. Polym. Chem. Ed.* **2000**, *38*, 2979–2992.

[3] a) K. S. Lee, C. G. Oh, J. H. Yim, S. K. Ihm, *J. Mol. Catal. A* **2000**, *159*, 301–308; b) T. Sano, H. Hagimoto, J. Z. Jin, Y. Oumi, T. Uozumi, K. Soga, *Macromol. Rapid Commun.* **2000**, *21*, 1191–1195; c) Z. S. Seddegi, U. Budrthumal, A. A. Al-Arfaj, A. M. Al-Amer, S. A. I. Barri, *Appl. Catal. A* **2002**, *225*, 167–176; d) M. Choi, R. Ryoo, *Nat. Mater.* **2003**, *2*, 473–476; e) H. Nakajima, K. Yamada, Y. Iseki, S. Hosoda, A. Hanai, Y. Oumi, T. Teranish, T. Sano, *J. Polym. Sci. Polym. Phys. Ed.* **2003**, *41*, 3324–3332; f) X. Dong, L. Wang, G. Jiang, Z. Zhao, T. Sun, H. Yu, W. Wang, *J. Mol. Catal. A* **2005**, *240*, 239–244; g) S. Spange, S. Grund, *Adv. Mater.* **2009**, *21*, 2111–2116; h) M. Choi, F. Kleitz, D. N. Liu, H. Y. Lee, W. S. Ahn, R. Ryoo, *J. Am. Chem. Soc.* **2005**, *127*, 1924–1932; i) C. Guo, D. Zhang, F. Wang, G.-X. Jin, *J. Catal.* **2005**, *234*, 356–363.

[4] a) K. Kageyama, J. I. Tamazawa, T. Aida, *Science* **1999**, *285*, 2113–2115; b) T. Uemura, S. Horike, K. Kitagawa, M. Mizuno, K. Endo, S. Bracco, A. Comotti, P. Sozzani, M. Nagaoka, S. Kitagawa, *J. Am. Chem. Soc.* **2008**, *130*, 6781–6788; c) M. Chen, H. Zhou, L. Zhou, F. Zhang, *Polymer* **2017**, *114*, 180–188; d) W. Kaminsky, A. Funck, C. Klinke, *Top. Catal.* **2008**, *48*, 84; e) Y. Lu, Y. Yang, A. Sellinger, M. Lu, J. Huang, H. Fan, R. Haddad, G. Lopez, A. R. Burns, D. Y. Sasaki, *Nature* **2001**, *410*, 913.

[5] a) R. Holst James, I. Cooper Andrew, *Adv. Mater.* **2010**, *22*, 5212–5216; b) Y. He, Q. Gui, Y. Wang, Z. Wang, S. Liao, Y. Wang, *Small* **2018**, *14*, 1800394; c) I. Píš, L. Ferrighi, T. H. Nguyen, S. Nappini, L. Vaghi, A. Basagni, E. Magnano, A. Papagni, F. Sedona, C. Di Valentin, S. Agnoli, F. Bondino, *J. Phys. Chem. C* **2016**, *120*, 4909–4918; d) S. Begum, Z. Hassan, S. Bräse, M. Tsotsalas, *Langmuir* **2020**; e) J. Maiz, J. Martin, C. Mijangos, *Langmuir* **2012**, *28*, 12296–12303; f) P. Sungjin, S. Choi Insung, *Adv. Mater.* **2009**, *21*, 902–905.

[6] a) S. Nair, P. Naredi, S. H. Kim, *J. Phys. Chem. B* **2005**, *109*, 12491–12497; b) S. Park, S. W. Yoon, K. B. Lee, D. J. Kim, Y. H. Jung, Y. Do, H. J. Paik, I. S. Choi, *Macromol. Rapid Commun.* **2006**, *27*, 47–50; c) B. Liu, S. Y. Jie, Z. Y. Bu, B. G. Li, *J. Mol. Catal. A* **2014**, *387*, 63–68; d) J. H. Lei, D. L. Li, H. H. Wang, Z. Q. Wang, G. Y. Zhou, *J. Polym. Sci. Polym. Chem. Ed.* **2011**, *49*, 1503–1507; e) J. H. Lei, D. L. Li, H. H. Wang, G. Y. Zhou, *Polymer* **2011**, *52*, 602–605; f) T. Wang, Y. Sun, L. Zhang, K. Li, Y. Yi, S. Song, M. Li, Z.-A. Qiao, S. Dai, *Adv. Mater.* **2019**, *31*, 1807876; g) J. Choi, B. Kang, H.-O. Kim, J.-S. Suh, S. Haam, J. Yang, *Nanoscale* **2019**, *11*, 2434–2438; h) L. Verstraete, B. E. Hirsch, J. Greenwood, S. De Feyter, *Chem. Commun.* **2017**, *53*, 4207–4210; Xu, Y. Zeng, C. Yu, F. Zhang, *J. Porous Mater.* **2020**, *27*, 95–105.

[7] K. Y. Choi, J. J. Han, B. He, S. B. Lee, *J. Am. Chem. Soc.* **2008**, *130*, 3920–3926.

[8] Z. Hu, C. Liu, Y. Wu, R. Liu, Y. He, S. Luo, *J. Polym. Sci. Polym. Phys. Ed.* **2011**, *49*, 812–817.

[9] a) T. Uemura, N. Uchida, M. Higuchi, S. Kitagawa, *Macromolecules* **2011**, *44*, 2693–2697; b) T. Uemura, N. Yanai, S. Kitagawa, *Chem. Soc. Rev.* **2009**, *38*, 1228–1236; c) T. Uemura, D. Hiramatsu, Y. Kubota, M. Takata, S. Kitagawa, *Angew. Chem. Int. Ed.* **2007**, *46*, 4987–4990; *Angew. Chem.* **2007**, *119*, 5075–5078.

[10] K. Wang, J. Lei, H. Nie, L. Shen, P. Chen, G. Zhou, *Macromol. Chem. Phys.* **2018**, *219*, 1800362.

[11] J. R. Jennings, J. E. Lloyd, K. Wade, *J. Chem. Soc.* **1965**, 5083–5094.

[12] J. W. Yoo, C. W. Lee, J. S. Chang, S. E. Park, J. Ko, *Catal. Lett.* **2000**, *66*, 169–173.

[13] a) J. D. Hoffman, R. L. Miller, H. Marand, D. B. Roitman, *Macromolecules* **1992**, *25*, 2221–2229; b) Q. Fu, B. Heck, G. Strobl, Y. Thomann, *Macromolecules* **2001**, *34*, 2502–2511.

[14] a) Y. Wang, Y. Lu, Z. Jiang, Y. Men, *Macromolecules* **2014**, *47*, 6401–6407; b) Y. Lu, Y. Wang, Z. Jiang, Y. Men, *ACS Macro Lett.* **2014**, *3*, 1101–1105.

[15] K. Wang, J. Lei, G. Zhou, *RSC Adv.* **2015**, *5*, 70703–70706.

Manuscript received: September 28, 2020
Revised manuscript received: October 20, 2020